ERCOFTAC Bulletin **44** *2000 pp.36–40*

Boundary layer control by means of electromagnetic forces

T. Weier, U. Fey, G. Gerbeth, G. Mutschke, V. Avilov
Forschungszentrum Rossendorf
P.O. Box 510119, D–01314 Dresden
GERMANY

1 Introduction

Control of flow separation by suction was first demonstrated by Ludwig Prandtl [1] together with the presentation of his boundary layer theory. Since that time, many active and passive techniques to control wall bounded flows have been developed. If the fluid is electrically conducting, an additional possibility of flow control is given by the application of a Lorentz force $\mathbf{f}$. This electromagnetic body force results from the vector product of the magnetic induction $\mathbf{B}$ and the current density $\mathbf{j}$:

$$\mathbf{f} = \mathbf{j} \times \mathbf{B}. \tag{1}$$

The current density is given by Ohm's law

$$\mathbf{j} = \sigma(\mathbf{E} + \mathbf{U} \times \mathbf{B}), \tag{2}$$

where $\mathbf{E}$ denotes the electric field, $\mathbf{U}$ the velocity, and σ the electrical conductivity, respectively. Depending on the conductivity of the fluid, one can distinguish between two different types of magnetohydrodynamic (MHD) flow control. If the fluid has a high conductivity in the order of $\sigma \approx 10^6$S/m like liquid metals or semiconductor melts, an external applied magnetic field alone can have a strong influence on the flow. As described by the right term of Eq. 2 the interaction of the flow with the magnetic field causes electrical currents in the liquid. These currents again interact with the external field and generate the Lorentz force field as given by Eq. 1. Typical electrolytes like seawater possess a much lower electrical conductivity in the order of $\sigma \approx 10$S/m. Therefore, electrical currents generated by the $\mathbf{U} \times \mathbf{B}$ term are too small to produce a noticeable Lorentz force. In order to obtain current densities large enough for flow control purposes in electrolytes, an additional external electric field $\mathbf{E}$ has to be applied.

The idea to influence the boundary layer of a low conducting fluid by electromagnetic forces dates back to the 1960s [2]. Only recently, it has attracted new attention to control turbulent boundary layers [3, 4, 5, 6]. Several different force configurations have been investigated mainly with the aim to reduce the skin friction of turbulent boundary layers. The application of wall normal Lorentz forces has been studied experimentally by Nosenchuck and coworkers [3, 7]. They report local skin friction reductions by up to 90%. However, numerical simulations of comparable configurations by O'Sullivan and Biringen [8] and Crawford [9] have not shown this strong reduction. The use of wall parallel forces in streamwise direction was first proposed by Lielausis and Gailitis [2]. The influence of such a force on a turbulent boundary layer has been studied experimentally by Henoch and Stace [5] and numerically by Crawford and Karniadakis [6]. Both report a reduction of streamwise velocity fluctuations, but also an increase of the skin friction with applied Lorentz force. An oscillating wall parallel Lorentz force in spanwise direction has been the subject of a numerical study by Kim [10]. He found skin friction reductions by up to 30%.

The aim of the present article is to give a short overview of the experimental results obtained by the authors. The investigations are focused on the use of wall parallel Lorentz forces in streamwise direction to control a flat plate boundary layer and flow separation on hydrofoils.

2 Theory and Parameters

A streamwise Lorentz force can be generated by a stripwise arrangement of electrodes and permanent magnets of alternating polarity and magnetization, respectively. Fig. 1 shows a sketch of such a geometry. If one assumes both electric and magnetic fields to have components in y and z direction only and neglects the induced currents $\sigma(\mathbf{U}\times\mathbf{B})$ compared to the applied one $\sigma\mathbf{E}$, the cross product $\mathbf{j}\times\mathbf{B}$ has an x component only. For given magnet configuration the distribution and the amplitude of the force can be determined by the polarity of the electrodes and the magnitude of the current density. That means also time dependent forces can easily be applied by just feeding an appropriate current to the electrodes. However, electrochemical aspects like the production of electrolytic bubbles have to be considered.

The concept of Gailitis and Lielausis [2] proposed to use a streamwise Lorentz force to stabilize a laminar flat plate boundary layer. A tremendous reduction of skin friction will result from transition delay, since turbulent skin friction in general is orders of magnitude larger than laminar one. The force distribution produced by the stripwise geometry shown in Fig. 1 can be calculated by series expansions of the magnetic and electric fields. As already found by Grienberg [11] the resulting force decays in a good approximation exponentially with the wall distance y. Considering also higher terms, a variation of the force density with the spanwise coordinate z appears. This variation arises from the singularities of the equations for the magnetic and electric field at the corners of the magnets and electrodes, respectively. In Fig. 2 the distribution of the Lorentz force calculated by the finite element Maxwell solver OPERA is shown. An exponential decay away from the wall, but also the distinct maxima of the force caused by the singularities are clearly visible.

Averaged over the spanwise coordinate z, the mean force density is given as

$$F = \frac{\pi}{8} j_0 M_0 e^{-\frac{\pi}{a}y}. \tag{3}$$

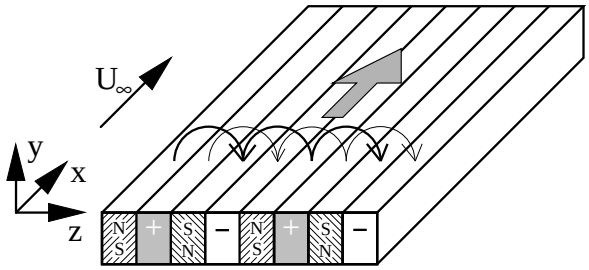

Figure 1: Sketch of the electric (thin) and magnetic (thick) fields and the resulting Lorentz force (gray arrow) over a flat plate

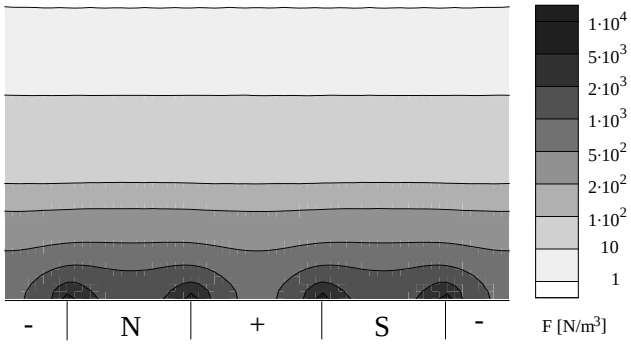

Figure 2: Calculated Lorentz force distribution

Whereby M_0 denotes the magnetization of the magnets. Magnets and electrodes have the same width a. Following the approach of Tsinober and Shtern [12], the boundary layer equations with electromagnetic force term may be written as

$$\begin{aligned} u\frac{\partial u}{\partial x} + v\frac{\partial u}{\partial y} &= -\frac{1}{\rho}\frac{dp}{dx} + \nu\frac{\partial^2 u}{\partial y^2} + \frac{\pi}{8}\frac{j_0 M_0}{\rho}e^{-\frac{\pi}{a}y}, \\ \frac{\partial u}{\partial x} + \frac{\partial v}{\partial y} &= 0. \end{aligned} \tag{4}$$

As usually, u denotes the streamwise component of the velocity and v the wall normal one. ρ is the fluid density and ν its kinematic viscosity. After normalization of equation (4) with the velocity of the outer flow U_0 and the electrode spacing a, a nondimensional parameter

$$Z = \frac{1}{8\pi}\frac{j_0 M_0 a^2}{\rho U_0 \nu} \tag{5}$$

appears describing the ratio of electromagnetic to viscous forces. It corresponds to the square of the Hartmann number if one compares it with usual MHD flows.
For the canonical case of a flat plate boundary layer, the streamwise pressure gradient dp/dx is zero. Provided $Z = 1$, the boundary layer thickness reaches an asymptotic value. That means, the momentum loss due to the wall friction is just balanced by the momentum gain caused by the electromagnetic force. In consequence an exponential boundary layer profile

$$\frac{u}{U_0} = 1 - e^{-\frac{\pi}{a}y} \tag{6}$$

develops which is similar to the asymptotic suction profile. This profile has a two orders of magnitude higher critical Reynolds number than the Blasius profile [13], so transition will be delayed considerably.
Flow separation occurs according to Prandtl [1] when fluid decelerated by friction forces is exposed to an adverse pressure gradient stronger than the remaining kinetic energy of the fluid. The boundary layer separates from the wall and a recirculation region forms. In consequence form drag increases and possible lift decreases.
To prevent separation, the momentum deficit of the boundary layer has to be overcome and the pressure gradient of the outer flow has to be balanced. Experimental demonstration of separation prevention on a circular cylinder by means of a streamwise Lorentz force with accompanying numerical simulations have been given in [14].
The normalization of the full Navier–Stokes equations leads to an additional nondimensional parameter

$$N = \frac{j_0 B_0 L}{\rho U_0^2}. \tag{7}$$

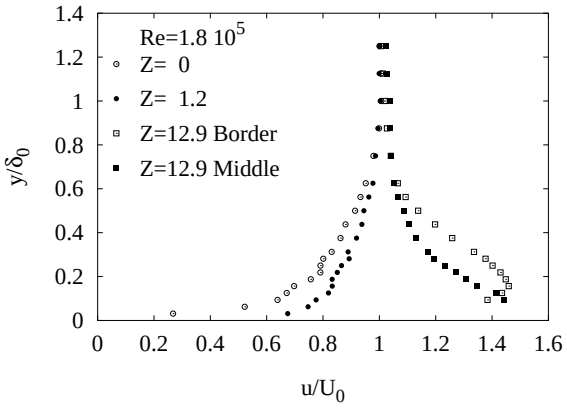

Figure 3: Mean velocity profiles for the flat plate boundary layer in parallel flow.

N is the so–called interaction parameter giving the ratio of electromagnetic to inertial forces. B_0 is here the surface magnetization of the permanent magnets and L is a characteristic length equal to the chord length c in the case of hydrofoils. Obviously N, Z and Re are not independent, since $Z/N \sim Re$.

3 Experimental Results

3.1 Flat Plate

The flat plate boundary layer measurements were carried out at the Hamburg Ship Model Basin (HSVA). As electrolyte aqueous sodium chloride with a concentration of 3.65% was used throughout the experiments. It has an electrical conductivity of approximately 5S/m. LDA measurements of the flat plate boundary layer took place in the medium cavitation tunnel. The plate has 25 electrodes and 25 magnet strips, each 10mm in width. The magnet/electrode array starts at 100mm from the leading edge of the plate and has a length of 400mm. Overall, the plate measures 500mm×590mm and was mounted in the middle of the tunnel. Leading edge and trailing edge are rounded. The magnets generate an induction of 0.35T at their surface and consist of neodymium–iron–boron (NdFeB). The electrodes are made from stainless steel.
In a second series of experiments the total drag of the plate has been measured by means of a force balance. These measurements have been carried out at HSVAs arctic environmental test basin. A more detailed description of the experimental equipment can be found in [15].
The effect of a streamwise Lorentz force on the mean velocity profile of a flat plate boundary layer is shown in Fig. 3. This profile was measured at the downstream end of the electrode/magnet array, i.e. at $x = 500$mm with x measured from the leading edge. The wall distance is normalized with the boundary layer thickness of the unforced boundary layer δ_0. A Reynolds number $Re = U_0 x/\nu$ of $1.8 \cdot 10^5$ slightly below the theoretical transition value characterizes the flow. As can be seen from the fluctuating velocities in Fig. 4 without the Lorentz force ($Z = 0$) the boundary layer flow is not laminar as it could be expected for such non–optimized conditions. A similar conclusion can be drawn by looking closer at the mean velocity profile, which is an intermediate profile between a Blasius and a logarithmic one. This early transition of the boundary layer is probably caused by the high turbulence level of 2% in the cavitation tunnel.
Thus the streamwise Lorentz force is, in contrast to the theory, applied to a turbulent boundary layer. For $Z = 1.2$ the influence of the force on the flow consists in a moder-

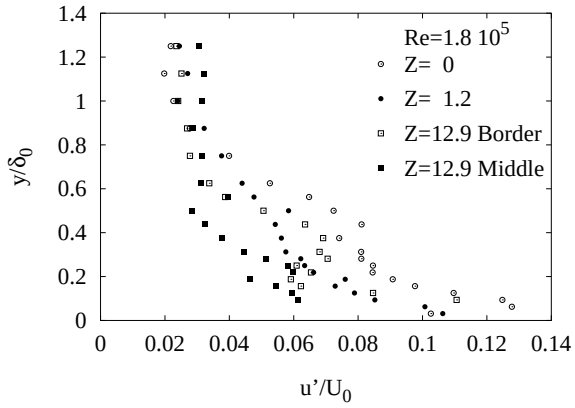

Figure 4: rms–values of the streamwise component for the flat plate boundary layer in parallel flow.

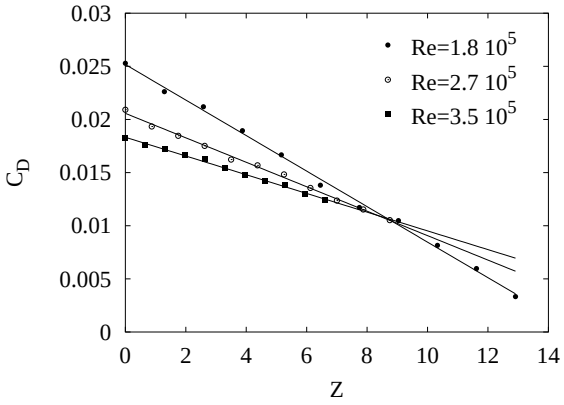

Figure 5: Coefficient of the total drag for the controlled flat plate

ate acceleration of the near wall fluid. The velocity profile becomes fuller, but its shape is not an exponential one. Mainly three reasons should be responsible for this behavior. At first, the early transition of the boundary layer causes conditions not considered in the theory. Second in order to establish the asymptotic profile, a certain evolution length has to be covered. A rough estimate can be given by looking at the definition of the dimensionless streamwise coordinate: $x' = \nu\pi^2 x/(a^2 U_0)$. x' should at least be in the order of 1 to allow the asymptotic profile to develop. An integration of the boundary layer equations show that at $x' = 7$ the boundary layer profile for $Z = 1$ has still a mean deviation of 1% from the exponential shape. The profiles in Fig. 3 are taken at $x' = 0.13$, i.e. at a position far from the required one. Third, the real force distribution differs from the ideal one. Their z modulations could have instead of the desired stabilizing effect a destabilizing one by possibly triggering transition due to secondary instabilities.

Looking at the rms–values of the streamwise component a damping due to the applied force near the wall is found, an effect already described in the experiments of Henoch and Stace [5]. A strong acceleration, as caused by a favorable pressure gradient, has a relaminarizing effect on the flow [16]. Dissipation in the near wall region is increased and turbulence production is suppressed. Unlike the favorable pressure gradient, the Lorentz force acts mainly in the direct proximity of the wall, therefore generating additional velocity gradients away from the wall. Further increase of Z up to 12.9 results in an increase of the streamwise fluctuations in this region.

At $Z = 12.9$ the mean velocity profile shows the form of a wall jet, demonstrating the strong accelerating effect of the Lorentz force. Fig. 3 gives the flow profile at two distinct positions in the spanwise coordinate z, at the border of a magnet and an electrode and above the middle of a magnet. The result of the spanwise modulations on the velocity distribution is clearly to be seen. The flow is stronger accelerated at the force maxima than at the minima.

For $Z = 7.5$ and $Re = 3.7 \cdot 10^5$ one can observe a boundary layer of practically constant thickness over the whole length of the magnet/electrode array. Hereby, the profiles were measured at an electrode–magnet border where the Lorentz force has its maximum. Shtern [17] used the von Kármán hypothesis to determine a criteria for a turbulent boundary layer of asymptotic thickness. The modified Hartmann number $Z \approx 15$ which results from his approach if one uses the force formulation (3) corresponds relatively good to the experimental value, since the local Hartmann number in the experiment is larger than the averaged one of $Z = 7.5$. It is evident, that the Lorentz force necessary to balance turbulent losses will be higher than that needed in the laminar case.

Force balance measurements of the total drag of the flat plate are given in Fig. 5. C_D denotes, as usually, the total drag force acting on the plate normalized by the stagnation pressure and the area of the plate. It is clearly to be seen, that the momentum added by the body force predominates the skin friction increase due to the steeper velocity gradient at the wall. The same conclusion could be drawn from an integration of the velocity profiles in Fig. 3. In consequence one can find a maximum reduction of the total drag by more than 80%. However, this drag reduction is indistinguishable from thrust and the energy expenditure necessary to feed the electrodes exceeds by far the drag reduction.

3.2 Separation Control

The wall jet in Fig. 3 at $Z = 12.9$ indicates the strong momentum increase in the boundary layer due to the Lorentz force. Since boundary layer separation occurs owing to an energy deficit of the near wall fluid, the streamwise Lorentz force should be able to counteract separation.

Separation prevention by electromagnetic forces has been studied both at a small flat plate and two hydrofoils. Flow visualizations of the flow around the flat plate have been carried out by means of the hydrogen–bubble–technique. An open channel with a cross section of 200mm×200mm filled with a sodium hydroxide solution was used. The NaOH concentration was 0.8% giving an electrical conductivity of 2.5S/m.

Visualizations of the flow around an inclined flat plate are given in Figs. 6 and 7. The flow is from the left to the right. Fig. 6 shows the flow around the plate without Lorentz force at an angle of attack $\alpha = 18°$. Since the Reynolds number based on the plate length is small, i.e. $Re = 1.24 \cdot 10^4$, the flow separates laminar at the leading edge without reattachment. Because of the leading edge separation, the flow should be influenced already at the nose of the plate. Consequently, the magnet/electrode–array is placed just behind the half cylinder forming the leading edge of the plate.

The flow situation under the influence of a Lorentz force of $N = 6.87$ is shown in Fig. 7. As the bubble strips indicate, the boundary layer is attached over the whole length of the plate. Due to the pressure rise in the outer flow, the boundary layer fluid is strongly decelerated at the leading edge. By the Lorentz force, the near wall fluid is sub-

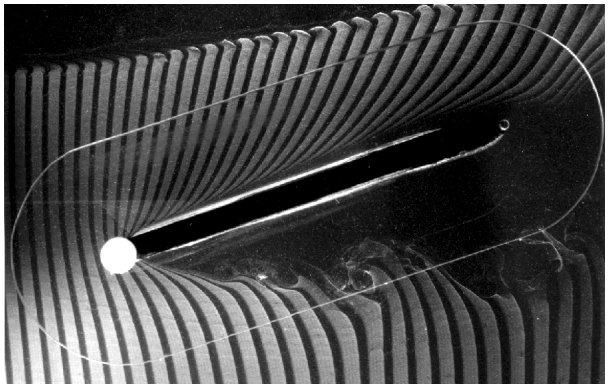

Figure 6: Inclined plate: Lorentz force off

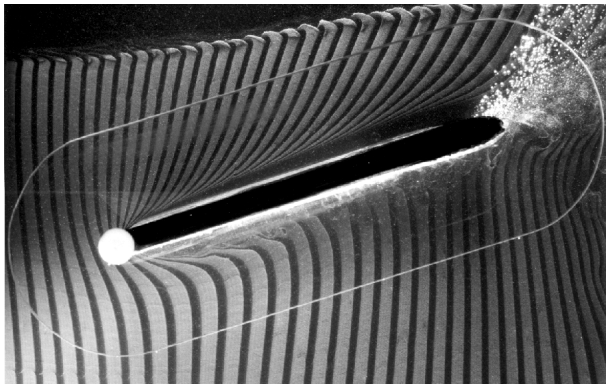

Figure 7: Inclined plate: Lorentz force on

jected to an acceleration while passing the plate. This can be seen by looking at the shape of the hydrogen bubble stripes near the plate.
A couple of larger bubbles leave the plate at the trailing edge. These big bubbles are formed by the electrolysis at the electrodes. The influence of the bubble motion on the flow is significantly reduced, if the velocity of the outer flow is increased because the increasing shear stress limits the maximum bubble size.
Separation of flow causes a form or pressure drag on the moving body simply due to the pressure difference between forward and backward stagnation point. This form drag estimates practically the total drag of bluff bodies at higher Reynolds numbers. Separation prevention can reduce the form drag to zero. The application of a streamwise Lorentz force for separation prevention has two additional consequences on the drag. On one hand due to the exponential force distribution, the velocity gradient at the wall and therefore wall friction is increased. On the other hand, the force exerts thrust on the body. At high enough forcing parameters a configuration is possible, where thrust overcomes drag.
Force balance measurements to determine drag, lift and pitching moment of two hydrofoils have again been carried out at HSVAs arctic environmental test basin. The same sodium chloride solution as in the flat plate experiments served as electrolyte. The PTL IV hydrofoils have a shape relatively similar to a NACA–0017 profile. Detailed information on the geometry is given in [15]. Both hydrofoils span width and chord length was $s = 360$mm and $c = 159$mm, respectively. The electromagnetic system of both plates differ in terms of electrode width a, surface induction B_0 and electrode material.
In Fig. 8 drag values of the PTL IV hydrofoil with $a/c = 0.03$ are presented for a Reynolds number $Re = 4 \cdot 10^4$ and different N versus the angle of attack α. The drag coefficient is defined in the usual way as

$$C_D = \frac{F_D}{\frac{\varrho}{2} U_0^2 cs}, \tag{8}$$

with F_D denoting the total force in streamwise direction as obtained directly from the force balance measurements. The Lorentz force in Fig. 8 acts on the suction side of the hydrofoil only. At the low Reynolds number considered here, separation occurs for $N = 0$ like at the flat plate as leading edge separation, but at an higher inclination angle of 13°. Since the separation occurs abruptly, a stepwise increase of the drag coefficient follows. The application of the Lorentz force at the suction side results for small angles of attack, i.e. in a situation without separation, in a decrease of the drag coefficient due to the momentum gain caused by the force. The drag reduction is relatively moderate ($\Delta C_D = 0.024$ at $N = 0.288$ and $\Delta C_D = 0.037$ at $N = 0.845$). A larger effect on the drag results from the separation delay. At $N = 0.288$ separation is postponed to $\alpha = 14.7°$ thereby C_D is reduced by $\Delta C_D = 0.044$. At $N = 0.845$ separation occurs first for $\alpha > 16.6°$, resulting in a $\Delta C_D = 0.084$.
Especially on a hydrofoil, separation doesn't influence the drag alone, but also the lift. Fig. 9 shows the lift lift coefficient versus the angle of attack at different interaction parameters N. Hereby, the lift coefficient is defined in

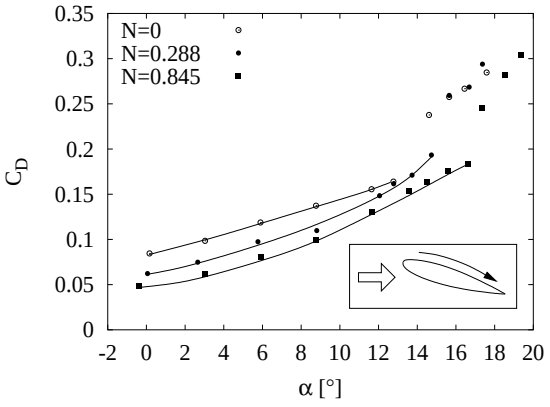

Figure 8: C_D versus α for $Re = 4 \cdot 10^4$, $a/c = 0.03$ and different interaction parameter.

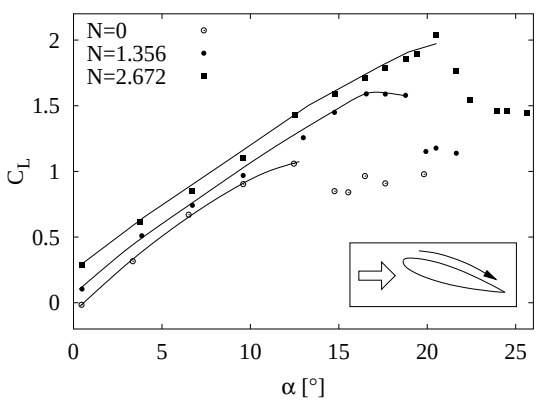

Figure 9: C_L versus α for $Re = 2.9 \cdot 10^4$, $a/c = 0.06$ and different interaction parameter.

analogy to the drag coefficient as

$$C_L = \frac{F_L}{\frac{\rho}{2} U_0^2 cs}. \quad (9)$$

Here F_L denotes the force on the hydrofoil in the direction normal to the oncoming flow. Fig. 9 gives experimental values obtained at $Re = 2.9 \cdot 10^4$ and $a/c = 0.06$. As in Fig. 8, the Lorentz force is applied at the suction side only. At $N = 0$ separation takes place at $\alpha = 13°$ leading to an abrupt lift decrease. If the Lorentz force is switched on, already at small angles of attack a lift increase can be seen. This lift increase results from the additional circulation caused by the acceleration of the suction side flow. Corresponding to the drag reduction at small angles of attack, also the lift increase due to the enhanced circulation is only moderate. Nevertheless it is possible to obtain a lift force even without an inclination of the hydrofoil.
A much larger lift increase results from the delayed separation of the suction side flow at high angles of attack. The lift coefficient increases further monotonically with growing angle of attack up to a point, where the Lorentz force is not any more able to withstand the pressure gradient of the outer flow. From Fig. 9 one can detect, that for the hydrofoil with $a/c = 0.06$ at $Re = 2.9 \cdot 10^4$ and $N = 2.67$ stall can be delayed up to $\alpha = 21°$. This results in an increase of the lift coefficient by 92% in comparison to the unforced flow.

4 Conclusion and Outlook

The influence of a streamwise Lorentz force on the flow along a flat plate has been studied in a saltwater flow. The experiments show a strong acceleration of the near wall flow if electromagnetic forces of sufficient strength are applied. The application of the streamwise force to the control of separation at an inclined plate and two hydrofoils has been successfully demonstrated. Stall is delayed to higher angles of attack resulting in an increase in maximum lift and a decrease in total drag of the hydrofoils.
Experiments on transition delay of a laminar boundary layer are scheduled for the near future. They will focus on the influence of the force inhomogeneities on the developing profile. On the other hand, experiments aimed to control flow separation at higher Reynolds numbers will be performed in order to determine the scale up of the approach.

Acknowledgment

Financial support from VDI under Grant NLD–FKZ 13N7134/1 and DFG under Grant INK 18/A1–1 is gratefully acknowledged. We would like to acknowledge Prof. Lielausis for fruitful discussions. Much appreciation goes to the team of the HSVA and to the Institute of Physics, Riga for their help in preparing the measurements.

Bibliography

[1] Ludwig Prandtl. Über Flüssigkeitsbewegung bei sehr kleiner Reibung. In *Verhandlg. III. Intern. Math. Kongr.*, pages 484–491, Heidelberg, 1904.

[2] Gailitis, A. and Lielausis, O. On a possibility to reduce the hydrodynamical resistance of a plate in an electrolyte. *Applied Magnetohydrodynamics. Reports of the Physics Institute*, 12:143–146, 1961. (in Russian).

[3] Nosenchuck, D.M. and Brown, G.L. Direct spatial control of wall shear stress in a turbulent boundary layer. In So, R.M.C., Speziale, C.G., and Launder, B.E., editors, *Near wall turbulent flows*, pages 689–698. Elsevier, 1993.

[4] Meng, J. C. S., Henoch, C. D., and Hrubes, J. D. Seawater electrohydrodynamics: a new frontier. *Magnetohydrodynamics*, 30(4):401–418, 1994.

[5] Henoch, C. and Stace, J. Experimental investigation of a salt water turbulent boundary layer modified by an applied streamwise magnetohydrodynamic body force. *Phys. Fluids*, 7:1371–1383, 1995.

[6] Crawford, C. H. and Karniadakis, G. E. Reynolds stress analysis of EMHD–controlled wall turbulence. Part I. streamwise forcing. *Phys. Fluids*, 9:788–806, 1997.

[7] Nosenchuck, D.M., Brown, G.L., Culver, H.C., Eng, T.I., and Huang, I.S. Spatial and temporal characteristics of boundary layers controlled with the Lorentz force. In *12^{th} Australian Fluid Mechanics Conference*, pages 93–96, Sydney, 1995.

[8] O'Sullivan, Peter L. and Biringen, Sedat. Direct numerical simulations of low reynolds number turbulent channel flow with EMHD control. *Phys. Fluids*, 10(5):1169–1181, 1998.

[9] C.H. Crawford. *Direct numerical simulation of near–wall turbulence: passive and active control*. PhD thesis, Princeton University, 1996.

[10] J. Kim. Boundary layer control for drag reduction: Taming turbulence. In G. Gerbeth, editor, *Int. Workshop on Electromagnetic Boundary Layer Control for Saltwater Flows*, 1997.

[11] E. Grienberg. On determination of properties of some potential fields. *Applied Magnetohydrodynamics. Reports of the Physics Institute*, 12:147–154, 1961. (in Russian).

[12] Tsinober, A. B. and Shtern, A. G. On the possibility to increase the stability of the flow in the boundary layer by means of crossed electric and magnetic fields. *Magnitnaya Gidrodinamica*, 3(2):152–154, 1967. (in Russian).

[13] Drazin, P. G. and Reid, W. H. *Hydrodynamic Stability*. Cambridge University Press, Cambridge, 1981.

[14] Weier, T., Gerbeth, G., Mutschke, G., Platacis, E., and Lielausis, O. Experiments on cylinder wake stabilization in an electrolyte solution by means of electromagnetic forces localized on the cylinder surface. *Experimental Thermal and Fluid Science*, 16:84–91, 1998.

[15] Weier, T., Fey, U., Gerbeth, G., Mutschke, G., Lammers, G., and Lielausis, O. Electromagnetic control of flow separation. In *2^{nd} Int. Conf. on Marine Electromagnetics*, pages 197–205, Brest, France, July 5–7 1999.

[16] K.R. Sreenivasan. Laminarescent, relaminarizing and retransitional flows. *Acta Mechanica*, 44:1–48, 1982.

[17] A.G. Shtern. Feasibility of modifying the boundary layer by crossed electric and magnetic fields. *Magnitnaya Gidrodinamika*, 6(3):124–128, 1970.